Caving 2022 - Y Potvin (ed.)

doi:10.36487/ACG_repo/2205_47

Controlled reopening of the Kiirunavaara production block 22 after a 4.2 magnitude event

M Svartsjaern *Itasca Consultants AB, Sweden*

T Rentzelos *Itasca Consultants AB, Sweden*

G Shekhar *LKAB, Sweden*

E Swedberg *LKAB, Sweden*

M Boskovic *LKAB, Sweden*

Y Hebert *Itasca Australia Pty Ltd, Australia*

Abstract

Large magnitude seismic events are a concern for most hard rock underground mines extracting minerals at depth. At the Kiirunavaara Mine, a long-term chain of events was initiated with a 3.0 magnitude event in 2008 in production block 19 on mining level 907 m. In the aftermath of the event, this production block started to trail behind the adjacent mining blocks creating an upward pointing wedge over three blocks, with block 19 at the top. In 2020 another large magnitude event (4.2 Mw) occurred in the same block, now designated block 22, while opening level 1022 m. The event caused significant damage to the mine infrastructure over a large volume affecting overall mine output for months.

Because of the significant damage to the infrastructure, it was not possible to resume mining on the topmost levels in block 22. Mining resumed instead from the lower levels, creating a remnant pillar between the existing sublevel and the resumed cave. The behaviour of this pillar has been analysed in detail using a coupled FLAC3D-CAVESIM numerical model. The modelling used a global-local approach where the mine scale stress field from sublevel cave mining until 2020 was superimposed on a local model where the resumption of mining activities in block 22 was explicitly simulated for several alternative layouts and sequences.

To alleviate the seismic hazard from an uncontrolled pillar collapse after resumed mining, the best option sequence was sought to facilitate controlled pillar caving. Variation studies were performed to find high impact parameters controlling the pillar behaviour. Parameters studied included looking at rock mass quality, horizontal sequencing and alterations in the footprint of the resumed cave.

From the modelling effort, it was concluded that the confinement of the remnant pillar was the major factor controlling the pillar caving and seismic potential. With support from underground damage assessments and the numerical models, it was decided to attempt to resume the mining from level 1079 m (abandoning the damaged levels 1022 and 1051). A new set of footwall drives were excavated inside the orebody to replace the damaged drives at the footwall contact. From the new footwall drives, the existing crosscuts were rehabilitated towards the old footwall drive as far as possible to reduce the confinement of the remnant pillar above. Resuming production at 1079 will attempt to reset the global mining sequence, with the production block no longer lagging compared to adjacent blocks.

Keywords: *numerical modelling, SLC, cave initiation, mine seismicity*

1 Introduction

The Kiirunavaara Mine is a sublevel cave (SLC) mine in the north of Sweden. The mine has an annual production of about 28 Mt, with the deepest extraction point at about 1,000 m depth from ground surface. The mine is divided into production blocks (BL for short). The block designations are based on the relative

block centroid Y-coordinate along the mine strike. BL 15–45 has a historical direct connection to the old open pit, while BL 12 and northward (area known as the Lake ore) is mined under a progressively caving crown pillar.

Like many other hard rock mines mining at depth, large magnitude seismic events are a concern, which is rising in severity as the mining progresses. At the Kiirunavaara Mine, a long-term chain of events was initiated in 2007–2008, with a 3.0 magnitude event in 2008 in production BL 19 on mining level 907 m. The event was tragically associated with a fatality prompting the mine to install a dedicated seismic monitoring system in late 2008 (Dahnér et al. 2008), which was significantly expanded in 2013 and 2019. Because of the severity of the 2008 event, the production of BL 19 was paused for a significant time period before any mining in the area was resumed, leading to the block lagging behind the adjacent mining blocks, thus creating an upward pointing wedge over three blocks with BL 19 at the top. In 2020 another large magnitude event (4.2 moment magnitude) occurred in the same block, now designated BL 22, while opening level 1022 m (four levels below the previous major event). The event caused significant damage to the mine infrastructure over a large volume affecting the overall mine output for months. The time has now come to resume mining in the affected blocks, and the steps taken to make this possible are outlined in this paper.

2 Background

2.1 Geology

The main geological model constitutes the orebody boundary (Ore), two diabase dykes (DB), clay alterations (clay), porphyry dykes (QP & DP) and host rock (varying types of trachyandesites or syenite and quartz porphyries), which are shown for the full mine width and for the local BL 15–26 in Figure 1. Estimated rock mass properties are given in Table 1; clay volumes are in a varied state of alteration but mainly occur south of BL 26 and were not included in the analyses of reopening BL 22.

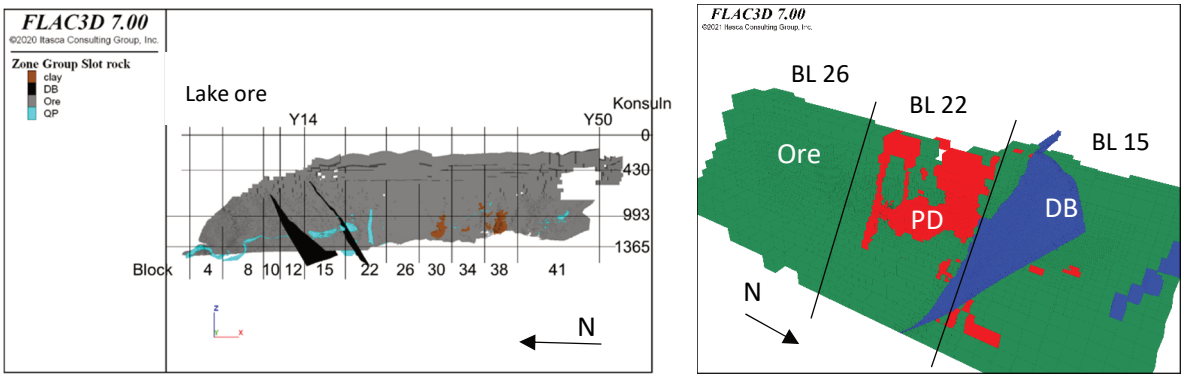

(a) (b)

Figure 1 Main geological entities. (a) Full mine view from footwall; (b) Production blocks 26 (from left), 22 and 15 (to right) in a view from the hanging wall for levels 760–1400 m

2.2 Mining front prior to the 2020 event

The production block 22 had, in 2020, for several years been trailing behind the adjacent BL 26 and 15. The orebody in BL 22 is also more narrow and geologically complex than the adjacent blocks leading to the block being mined using a single longitudinal production drift on level 993. The adjacent blocks on both sides have been mined with transverse crosscuts on the same level, see Figure 2. This, together with BL 22 trailing behind the adjacent blocks, has resulted in a relative increase of all principal stress components in BL 22 compared to BL 15 and 26.

Table 1 Estimated rock mass parameters for main geological units

Property	Footwall	Hanging wall	Ore	Diabase (DB)	Quartz-porphyry (PD)	Cave and blasted rock
Density (kg/m^3)	2,800	2,800	4,600	2,800	2,800	2,800
Intact Young's modulus (GPa)	65	42.5	60	65	65	0.2*/0.28*
UCSi (MPa)	180	225	183	175	320	–
GSI	76	66	67	44	81	–
mi	20	18	17	15	20	–
Residual friction angle (°)	30	30	30	30	30	43**
Dilation angle (°)	10	10	10	10	10	–

** Cave rock was modelled using ideal-plastic Mohr–Coulomb using E/v; ** Internal friction angle*

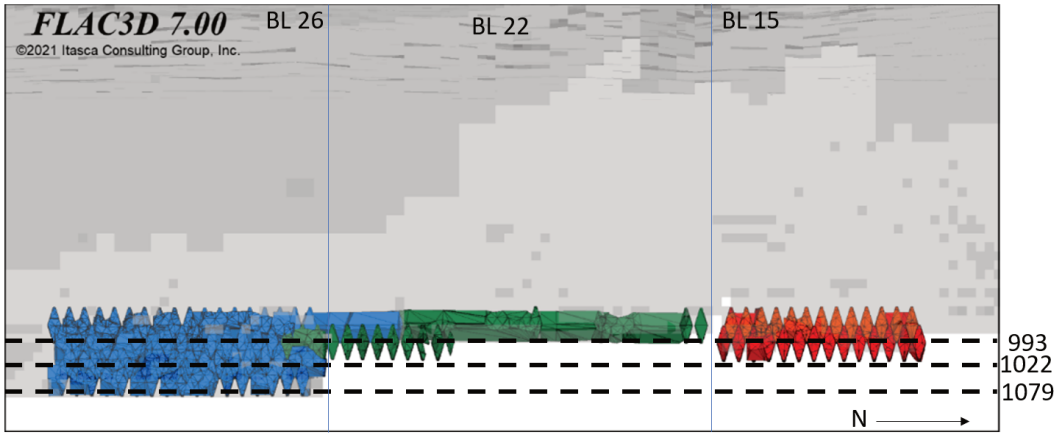

Figure 2 Simplified historic mining sequence until mining year 2020. BL 26 (blue), 22 (green) and 15 (red) mining fronts with approximated SLC cave in light grey, view from the hanging wall

3 Block 22 seismic event in May 2020

On 18 May 2020, at 03:11 local time, a large seismic event with the hypocentre location in BL 22 was registered. The seismic event was the largest ever recorded in the mine. It was recorded by all seismic sensors in the mine, the 1 Hz seismic sensors at Malmberget Mine, 120 km away, and by the regional seismic stations up to a few thousand kilometres away from the mine. The moment magnitude of the event was estimated as 4.2 ± 0.2 by using data from the regional seismic stations, as the in-mine system could not correctly record the low frequency spectra of the event.

The seismic event was very complex; it started with the shorter small-amplitude phase from which it could be identified by P- and S-arrivals. That phase was followed by a more intensive and much longer phase in which no P-arrivals could be identified, and S-arrivals were much stronger.

3.1 Event localisation

Due to signal saturation of the local seismic system, the regional seismic system was mainly used to estimate the magnitude; however, the in-mine system was used to estimate the hypocentre location. Several methodologies were used to calculate this point, and a comparison of the results showed statistically insignificant differences, less than 10 m, in the horizontal plane while slightly larger differences, up to 25 m, in depth. Because of the complexity of the seismic event and the size of the event, the hypocentre location

should be considered as the initiation point of the large event. The hypocentre location was determined from processing by the Institute of Mine Seismology (IMS), to be at -1148 m depth and in the vicinity of ore pass 221 as shown in Figure 3.

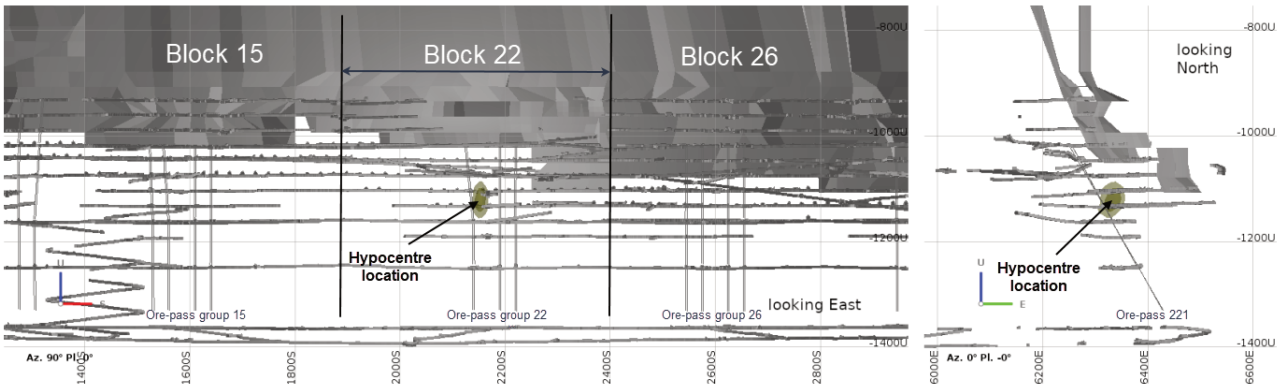

Figure 3 Location of the hypocentre (initiation point) of 18 May 2020, seismic event, with the 68% and 95% confidence regions (modified from Malovichko 2021)

3.2 Precursors and aftershocks

Analyses of seismic activity prior to the event on 18 May 2020, showed no clear pre-cursors to the event. An aftershock series started 15 seconds after the large event constituting about 36,000 events. The aftershocks were not symmetrically distributed around the large event, Figure 4, and they could be grouped in three clusters. In the first three days after the 18 May seismic event, there were no production blasts or any other activity in the mine.

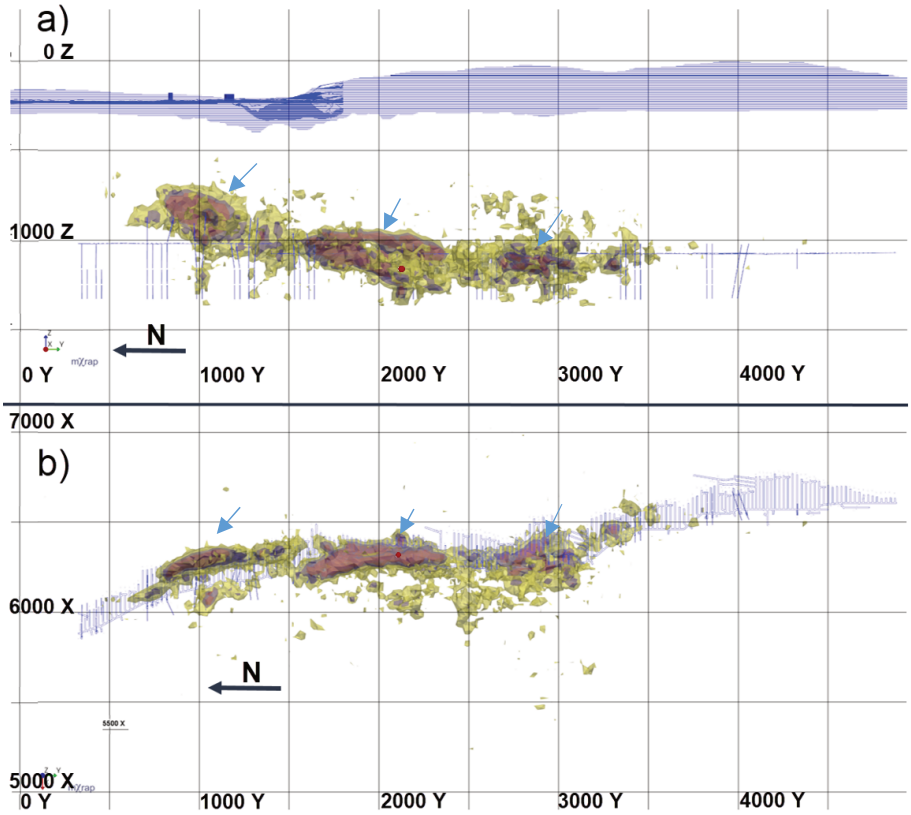

Figure 4 (a) Vertical view looking east of density iso-volumes of aftershocks during three days after the seismic event on 18 May 2020, marked with the red dot. Iso-volumes levels (events/10^6 m^3): (b) Top view of the same. Seismic clusters indicated by arrows and deliniated by iso-volumes

Seismic activity in the southernmost cluster began to decrease during the second day and ceased the third day after the main event. After production blasts resumed on 21 May in the north part of the mine, aftershocks were mixed with the blast response and difficult to separate. However, the cluster closest to the large event lasted the longest – it took almost one month before the seismic activity in that area was on the same level as before the seismic event on 18 May.

The spatial distribution of aftershocks correlates with the spatial pattern of the analysed strong ground motion of the large event. For aftershocks registered between Y1600 and Y3150 within the first 24 hours, the source mechanism analyses (Malovichko 2021) showed that:

- North of the large event's initiation location, between Y1600 to Y2050, aftershocks tend to cluster around the footwall drifts. The source mechanisms of these seismic events were of a crush-type with the P-axis (a proxy for σ1) oriented approximately orthogonal to the orebody.
- In the area close to the large event's initiation location, between Y2050 to Y2350, the aftershocks had a similar crush-type mechanism, but events were more scattered, with their P-axis slightly rotated to the north compared to the above.
- South of the large event's initiation location, between Y2350 to Y3150, the source mechanism of the aftershocks were a combination of slip-type and crush-type. The orientation of the P-axis was different from the previous two and plunged steeply to the East. The aftershocks were mostly located in the footwall.

3.3 Post event damage mapping

Inspections of the mine commenced on the day of the event and have been ongoing as areas have been recovered. For the first few days after 18 May 2020, the focus was to identify and close off the areas of the mine that were damaged during the seismic event. Areas of severe and moderate damage could therefore be delineated relatively quickly, as illustrated in Figure 5.

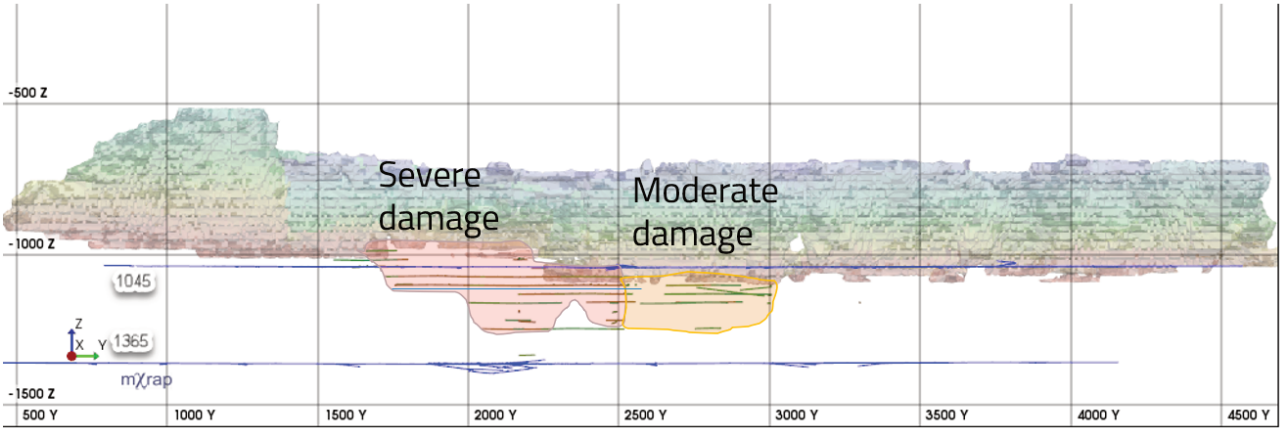

Figure 5 Section view of the mine looking from the footwall side, with shaded areas indicating severe damage (red hue) and moderate damage (yellow hue). The wireframe shows mined-out volumes as of 17 May 2020. The 1045 and 1365 m haulage levels are also shown in blue. One square is 500 × 500 m

Damage was classified using a Rock Damage Scale (RDS) and plotted on level plans (Figures 6 and 7). Two general observations that apply to all inspected areas are that the extent of damage was greatest in: (i) ore-parallel drifts; and (ii) drifts close to the orebody (i.e. the mined SLC). Also, the transition from complete collapse (R5) to no visible disturbance (R0) was, in most cases, very distinct. This was especially true for levels 1108 m and below.

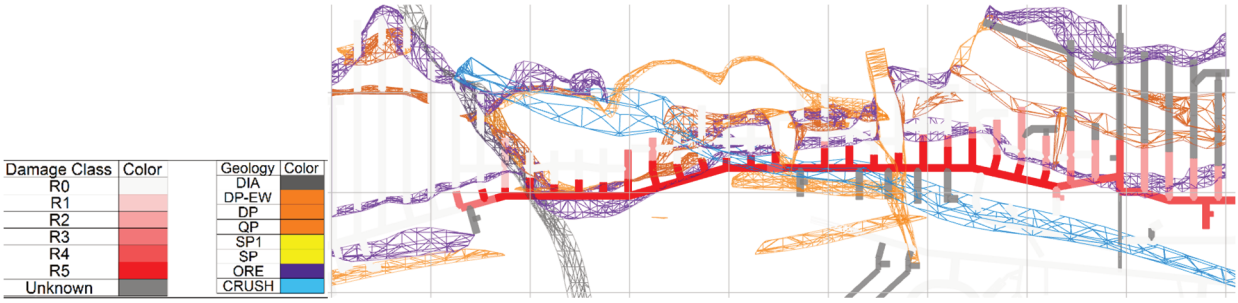

Figure 6 Plan view of level 1079 m, with damage plotted according to the RDS

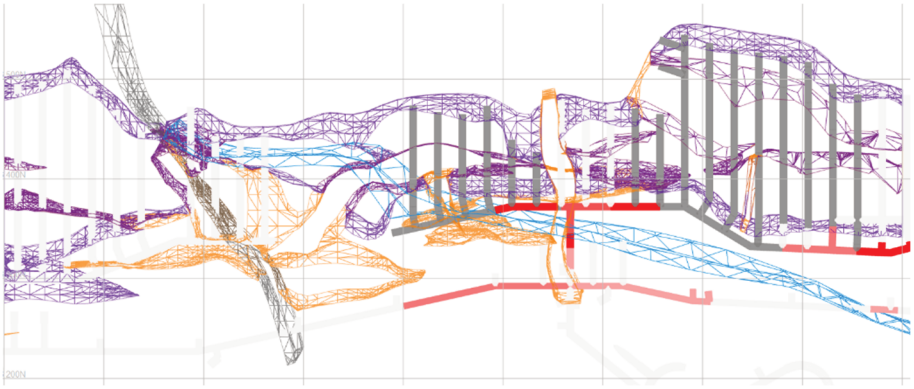

Figure 7 Plan view of level 1165 m, with damage plotted according to the RDS

The appearance of the damage varies depending on excavation geometry and the lithology in the area. It was possible to delineate at least two different categories: (a) dynamically triggered failure of over-stressed rock around excavations; and (b) large-scale failures in the rock mass (Figure 8).

(a) (b)

Figure 8 (a) Damage with rock pieces delineated by a combination of pre-existing structures as well as fresh failure surfaces. The original structure of the rock mass is no longer observable; (b) Damage where the displaced material has retained parts of the structural fabric but is visibly disturbed with clear rotation and translation of blocks

Based on the interpretation and locations of the observed damage, it is inferred that a major mechanism of damage was stress-driven failure due to the high tangential stress concentrated around the ore-parallel drifts close to the mined-out SLC. These failures were facilitated by the fact that two of the main joint sets in the mine run parallel to the orebody, creating the potential for deep (>10 m) structurally defined falls of ground.

4 Reopening alternatives

The resumption of production in the damaged area is dependent on selecting levels for creation of new footwall drifts in the damaged area. The new drives are located inside the orebody (as compared to the old footwall drifts located outside the footwall contact). After the seismic event, three levels were initially selected for rapid development of new footwall drifts, namely levels 1079, 1108 and 1137. Production levels 1022 and 1051 were not selected for development. This was becouse the southern block (BL 26) levels had already been mined, leaving access from only the north. After quantifying the level of continuous damage in the old footwall drifts from the initial development, it was decided that development at the levels above will not help to connect the cave. This conclusion was mainly based on the ore offset meaning that new footwall drifts would be located purely in waste rock as the orebody was thin at level 1022 and 1051. This left the mine with two alternatives for reopening the production in the damaged area; leaving a smaller pillar and opening at level 1079 (two level pillar), or leaving a bigger (three level) pillar and opening at level 1108 (Figure 9).

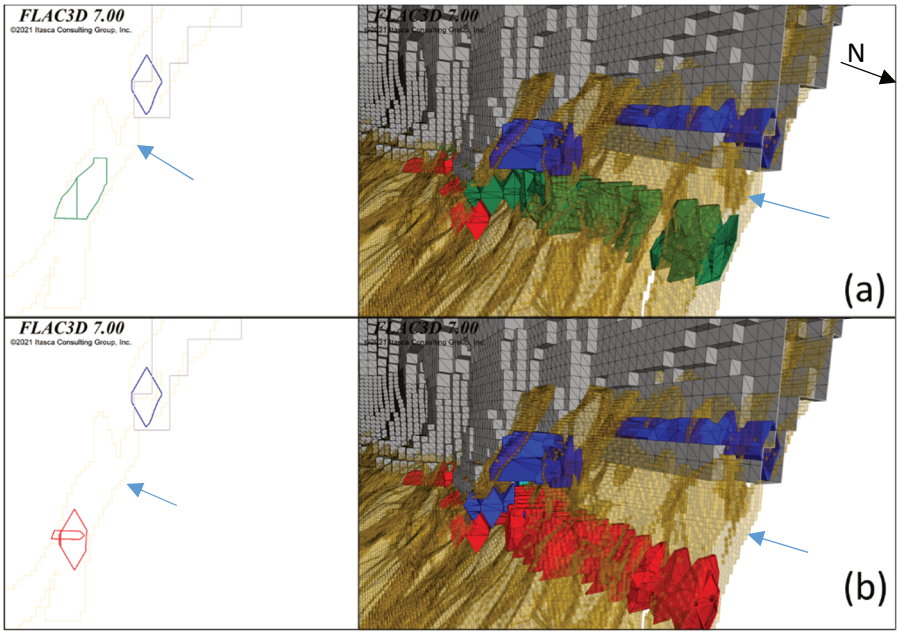

Figure 9 (a) Mining geometry mid-pillar when resuming from level 1079 (green), approximated SLC (grey), ore (orange) and mining front levels prior to resumption (blue); (b) Mining geometry mid-pillar when resuming from level 1108 (red). Pillar position indicated by blue arrow

4.1 Alternative mining plans for level 1079

Detailed life-of-mine plans (LOMP) were developed for both alternatives to help understand the effect on the global mining sequence and production for the mine. The LOMP was provided as input information for numerical modelling and analysis of the rock response. For each of the alternatives of resuming production at level 1079 or 1108, the mining sequences were designed to observe the effect of keeping either block 22 or 26 as the deepest point in the mining sequence.

The planning and analysis of rock mechanical response were done iteratively. The alternative mining plans were first ranked from a block scale perspective, and the best global sequences were then further analysed on a detailed (ring by ring) level. The three initial alternative plans were:

1. South to north: The mining resume from the southernmost drifts northward. Crosscuts are only rehabilitated between the new footwall drive (located in ore) and the hanging wall.
2. Middle and out: The mining resume from near the southern part of the block and opened both directions. The drifts where production start intersect with the QP intrusion. This sequence aimed

to highlight the difference between mining from the intrusion compared to towards the intrusion as was done in alternative 1.

3. North to south: The mining resumes from the north towards the south. The mining follows the geometry and tries to open as close to the diabase intrusion as possible and mine towards the south part of the block.

Two successive mine plans were also created after the three above alternatives had been analysed. The fourth sequence looked at the effect of mining two levels at a time while maintaining an offset between the levels. The fifth sequence looked at mining as much as possible from the damaged levels by rehabilitating the crosscuts between the old and the new footwall drifts.

4.2 Rock response

4.2.1 Numerical model set-up

The rock mechanical aspects of the alternative reopening plans were evaluated using forward analysis by numerical modelling in *FLAC3D* (Itasca 2021). The modelling was focused on BL 15–26, with the problematic BL 22 in the middle. To accurately simulate the 3D stress field at blocks 15–26, a mine scale model was used for the LOMP evaluation. The full dimensions of the model were 4,500 m × 7,500 m × 1,600 m (Figure 10). A model depth of ≈1,600 m corresponds to mining level 1,600 m. The ground surface geometry was based on the 2017 LKAB digital terrain model with some simplifications. A total of four explicit slip planes were incorporated into the model simulating the weak contacts of the diabase dykes (one slip plane on each side of a dyke).

The rock mass units (Table 1) were modelled as *IMASS* (Itasca Constitutive Model for Advanced Strain-softening; Ghazvinian et al. 2020) materials except for the caved rock (when applicable), which was modelled as a frictional Mohr–Coulomb material.

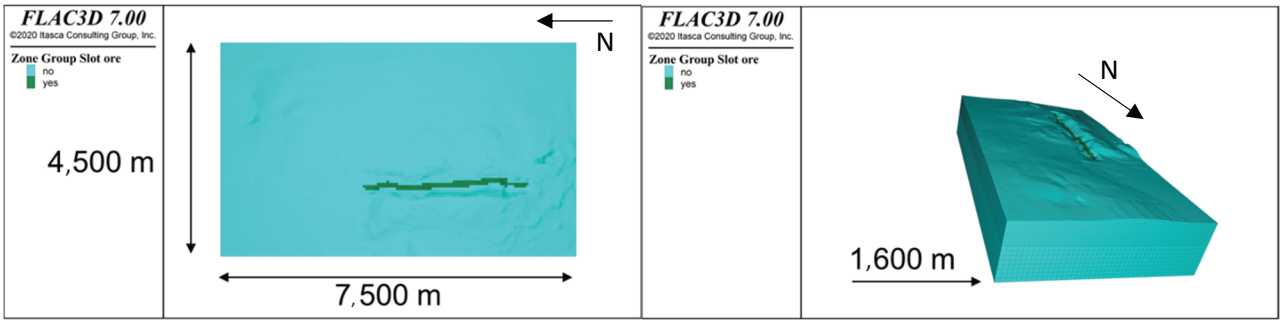

Figure 10 Global model dimensions for mine scale modelling of alternative LOMP

The initial stress state (prior to initial equilibrium) was based on the stress measurement compilation by Sandström (2003). Initial stresses on mining levels below 215 m were applied as follows (assuming zero stresses at the ground surface of the hanging wall at z = -200 m) with z decreasing towards the depth:

$$\sigma_H = 7.4 + 0.037z, \sigma_h = 5.6 + 0.028z, \sigma_v = 5.8 + 0.029z$$

where:

σ_H = major horizontal stress (most compressive) in MPa, orientated semi-perpendicular to the ore strike (east–west).

σ_h = minor horizontal stress (least compressive) in MPa, orientated semi-parallel to the ore strike (north–south).

σ_v = vertical stress in MPa.

Above level 215 m (z = -215), gravitational stresses were assumed for topological features such as the footwall peak. Compressive stresses are negative, displacements are positive when directed along the positive coordinate axis, normal strains are positive for extension, and volumetric strain is positive for volume increase.

4.2.2 Level 1051 remanent pillar entry level

The main rock mechanical aspect of reopening BL 22 is the level 1051 remnant pillar created by the permanent loss of level 1051 and major parts of level 1022 in the block. The geometry of the remnant pillar is complex. The practical width (horizontal extent between footwall and hanging wall) and thickness (vertical extent) vary significantly due to both historical mining above and planned mining below (Figure 11).

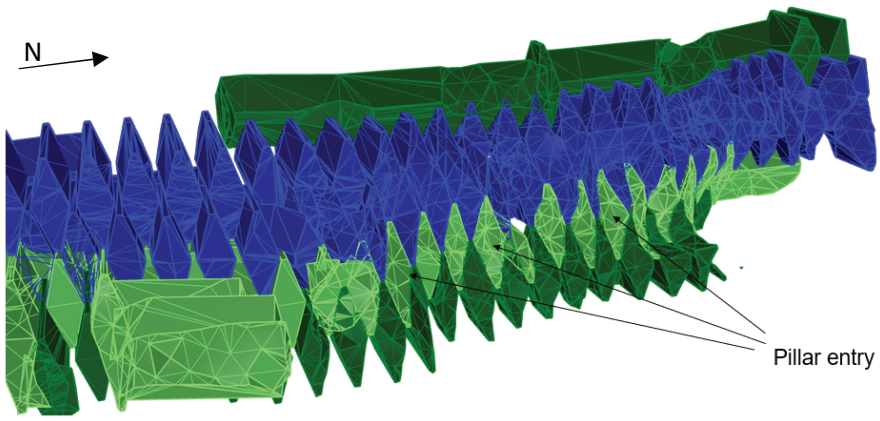

Figure 11 Isometric view of the pillar (blue) and undercut (light green) at level 1079 m and (dark green) at level 1108. Dark green above the pillar (blue) show mined area on level 993 m

From the start, the southern part of the pillar is already partially decoupled from the hanging wall due to partial mining on level 1022 in BL 22 during 2015. The global model suggests that the progression of pillar caving is similar regardless if the pillar is initially undercut from 1108 m or from level 1079 m. In both cases, the pillar collapses when the pillar is between 1 and 2 sublevels high. It was not possible with the present global model resolution to judge how the pillar would cave or if it would fail progressively or violently.

4.2.3 Detailed study of 1051 remnant pillar

In the global model, any remaining pillar between the old SLC and resumed production was assumed to cave into the resumed mining footprint as it was slashed from below. As indicated in Figure 12, the actual caving process during pillar mining could not be captured by the global model. A local model was created to explicitly investigate the 1051 remanent pillar behaviour during mining of levels 1079 and 1108 m, assuming a pillar entry at level 1079. The goal of the analysis was to find a sequence with the highest probability of controlled pillar caving to minimise the seismic risks.

For the local model code coupling between *FLAC3D* and *CAVESIM* (Sharrock 2021) was used to model the caving progression. In this methodology, two sets of models were prepared; a mechanical model in *FLAC3D* featuring all geomechanically relevant parameters, such as elastic and strength parameters for the rock mass for included entities (different rock types or geomechanical regions), as well as a block model in *CAVESIM* including material densities.

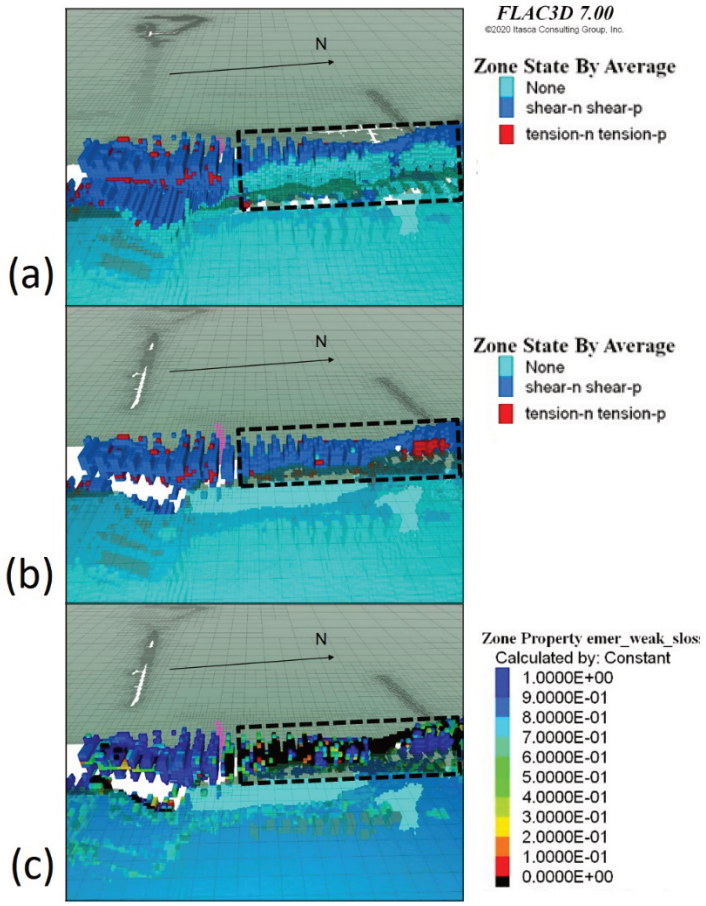

Figure 12 (a) Initial (intact) pillar during undercut at 1079 m (dashed black); (b) Pillar subjected to shear failure (dashed black) after overhand slashing of level 1051; (c) Pillar sloss contour after overhand slashing of level 1051, sloss = 0 indicate caved material. Note that host rock is shown in all figures (a–c) in a horizontal plane without yielding information

The caving process is represented by a by-directional coupling method between *CAVESIM* (Sharrock 2021) and *FLAC3D*, based on the method described by Hebert & Sharrock (2018). Production advance is simulated in *CAVESIM*, where material is drawn from the drawpoints based on the input draw schedule. Material flow is simulated within *CAVESIM*, and the resulting airgap volume and volumetric flow rate in the cave are communicated to the *FLAC3D* model. Within *FLAC3D*, the airgap is identified and removed from the system, and the stress state at the cave boundary is progressively reduced to account for the reduction in support provided by the muck pile during flow. The cave boundary is identified as caved material in contact with areas of the model that is not mobilised. As a result, the cave propagates within *FLAC3D*, and the new cave shape is sent to *CAVESIM*. This cycle is repeated until the end of the mining sequence in monthly increments.

The local *FLAC3D* model was a high-resolution geological clone of the global model. The local model shared coordinate system with the global model allowing the stress state in the global model for the mining step 2020 to be superimposed on the local model by retrieving the stress state from the global model for each zone centroid position in the local model, see Figure 13a. The local model included explicit infrastructure as well as an approximated 2020 cave from a separate mine scale caving model (Figure 13b).

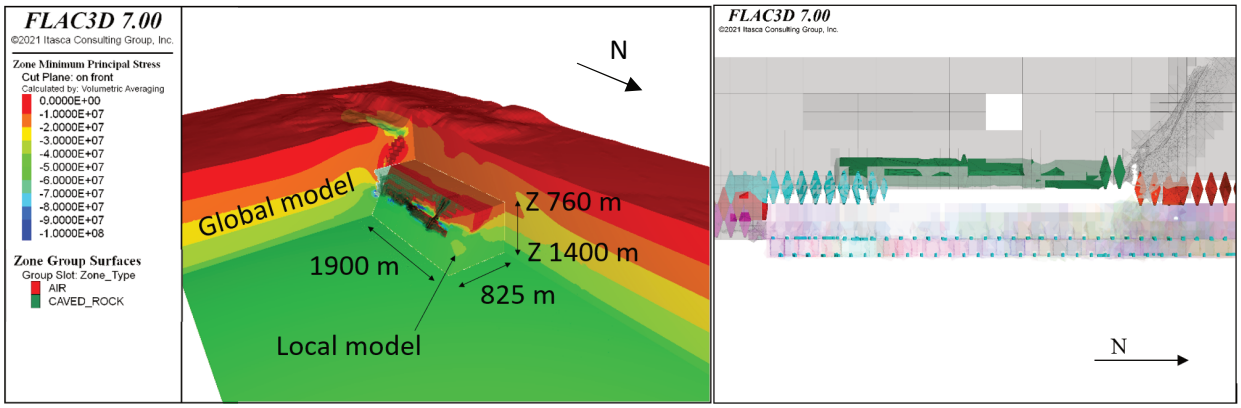

(a) (b)

Figure 13 (a) Superimposed stress state from global to local model; (b) Hanging wall view of mining front 2020 (diamonds) estimated SLC (grey) and planned local model production on levels 1079–1108, including planned blast (opaque). Note that mining on level 993 was performed using longitudinal SLC in BL 22 (green)

Undercut blasting from level 1079 m will with this plan reach as highest to level 1022 m effectively leaving a pillar between 1022 and the previously mined level 993 m. The offset means that the effective thickness of the un-blasted 1022 pillar will be larger than the vertical distance to level 993 (Figure 14). If blasting is successfully executed according to this plan, the remaining pillar will have a thickness of 30 to 50 m.

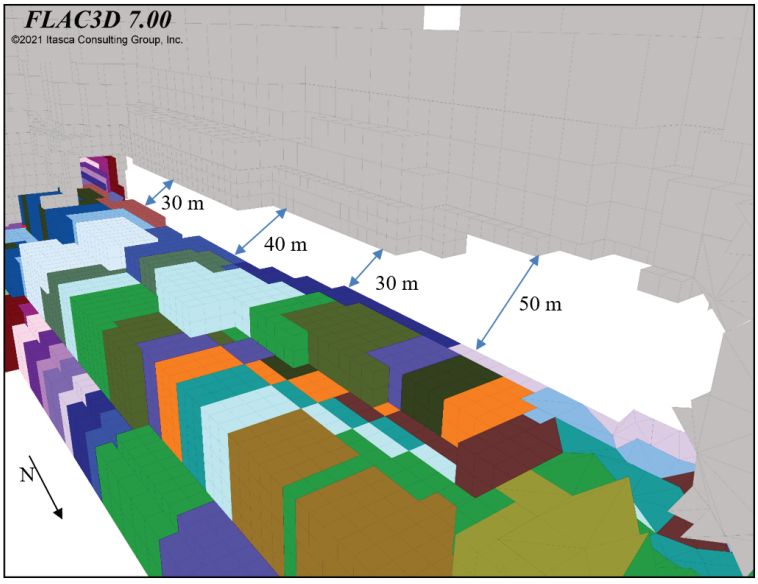

Figure 14 Close-up of un-blasted pillar between Y1740 and Y2250 including planned blasting up to level 1020 from 1079 m

As an alternative to the initial plans a larger footprint and smaller offset between the new and old cave was evaluated (Figure 15). The larger footprint was created by the rehabilitation of existing crosscuts on level 1079 towards the footwall contact. The purpose of doing this was twofold: (i) to increase the caveability of the cave back by expanding the footprint; and (ii) to allow for the pillar to be deconfined and thus weaken the pillar core by reducing the offset between the two caves.

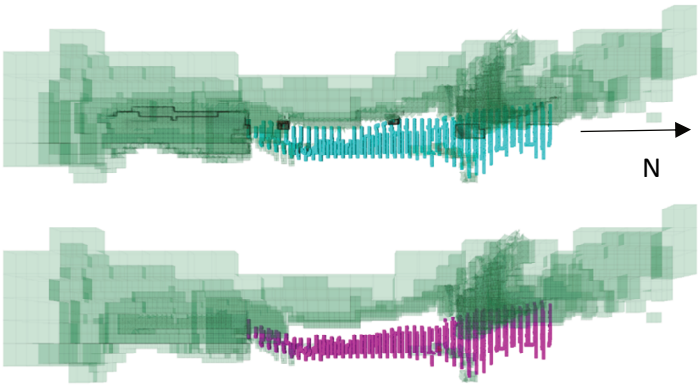

Figure 15 Top view of footprint (drawpoints) for rehabilitated crosscuts (upper) and mine plan from a global model (lower) in relation to (an approximated) existing cave (green)

The pillar confinement reduces significantly through the pillar centre for the extended crosscut plan compared to the initial plan. Mining was performed from the north towards the south for both sequences (with and without rehabilitated crosscuts). With the extended crosscuts towards the footwall contact, the pillar becomes initially unstable after mining past Y2150 with progressive pillar caving between Y1875 and Y2150, while pillar caving is inhibited without the extension of the crosscuts (Figure 16). A sensitivity analysis was performed where the rock mass quality (expressed as *GSI*-value) of the hanging wall was stepwise lowered from 66 to 56, this did, however, not affect the principal results.

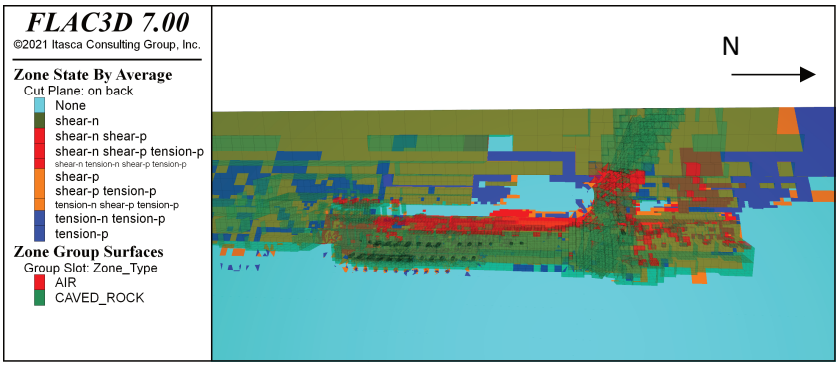

(a)

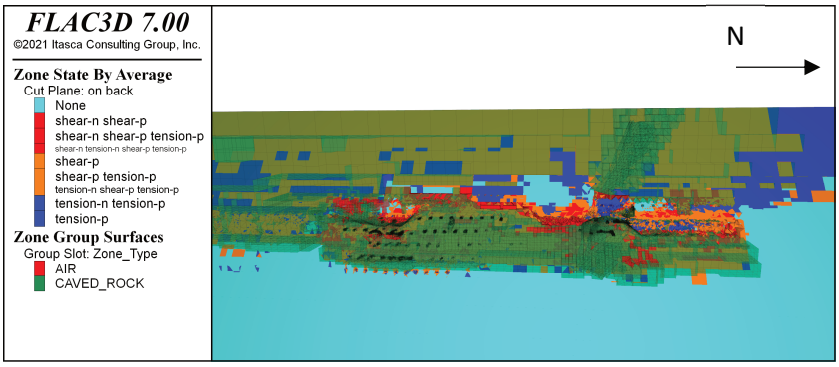

(b)

Figure 16 (a) 1051 remnant pillar without extended crosscuts; (b) Instability and progressive caving in the remnant pillar between Y1875 and Y2150 with extended crosscuts

4.3 Forward mining plan

Resuming production for the damaged area (Y17-Y25) was proposed at 1079 level based on the numerical modelling results. This mean that production is not performed at 1022 and 1051 in BL 22. The ore loss at

levels 1022 and 1051 are then partially retrieved as secondary and tertiary recovery from production at levels 1079 and 1108. Resuming production at 1079 aims to restart a new cave, which will be connected in the north and south with the global cave front and as mining continues deeper, the cave front will connect upwards with the narrow cave at level 993 and above. Figure 17 shows the schematic future mining sequence planned to be achieved by resuming production in block 22 at the 1079 level.

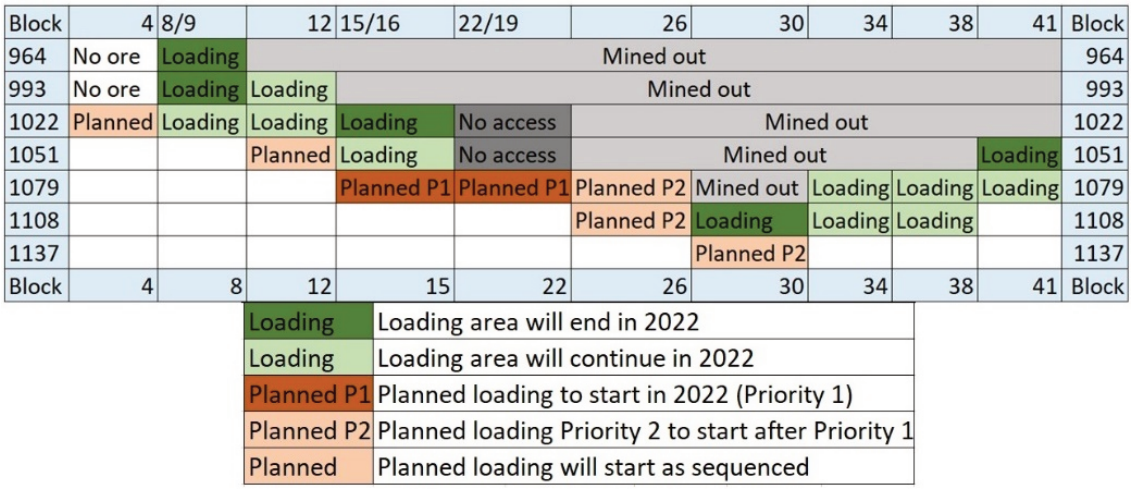

Figure 17 Schematic of future mining sequence

As shown in Figure 17, the restart of production in BL 22 directs the resumption of production in BL 26 and 30, which have been stopped to maintain the current mining front and not create more lag in the global mining sequence. Once the pillar is undercut at level 1079 and a uniform cave front is achieved at level 1079, production will be resumed in BL 26 and 30. The mining will start from north to south at level 1079, i.e. from BL 15 and going towards BL 22 to eventually connect with the cave at BL 26. Figure 18 shows a decision tree that shows the critical path for the selected mine plan.

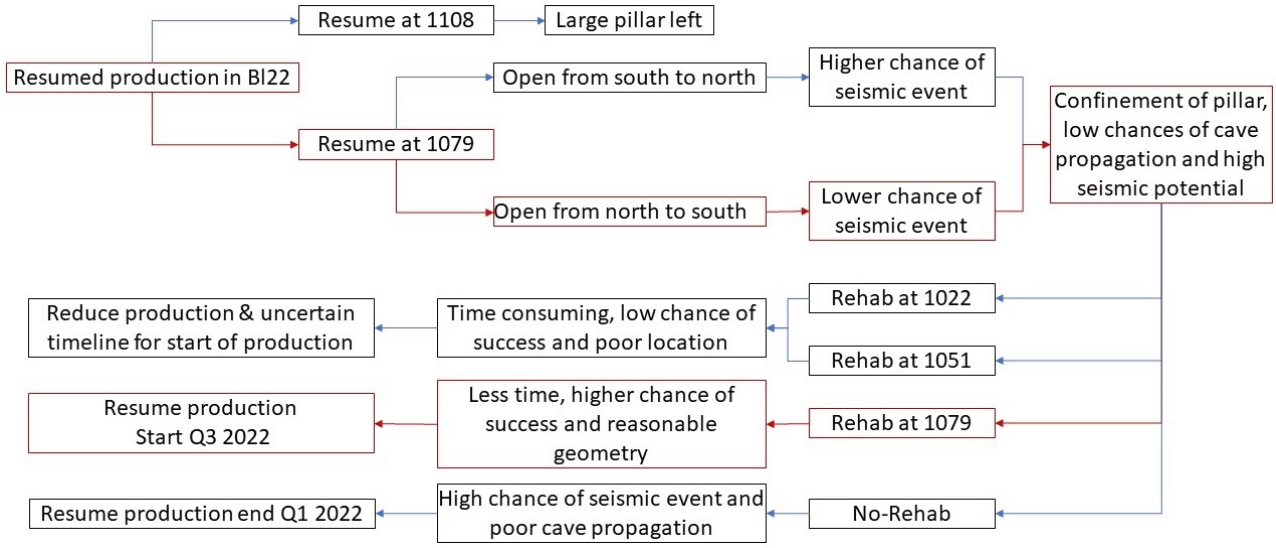

Figure 18 Decision tree showing the critical path for the selected mine plan

The three primary reasons for resuming production at level 1079 from the north to the south direction were:

1. Resuming production at 1079 for Y17–Y25 will reset the global mining sequence in the mine. BL 22 will not be lagging in sequence as was the case before the seismic event, and the global mine sequence will have a one-block one-level lag which is ideal to achieve a shallow 'V front' cave shape for the mine.

2. Resuming production at 1079 instead of 1108 will mean less material is left above the resumed production level. A restart at level 1079 provide a more controlled condition (as the pillar is smaller), which is more comparable to mining without a pillar. The smaller pillar dimension ensures that yielding occurs with mining advancement.
3. During the development of new footwall drifts at 1079, 1108 and 1137, the mine observed more seismic response when developing from north to south compared to the development performed from the south. This, along with other observations, point to higher stress in the northern part of the block; hence mining from a relatively higher stressed to a lower stressed region was the logical decision.

5 Conclusion

From the results of the analyses performed, the mine saw a need to rehabilitate as much as possible the crosscuts between new and the old footwall drives to facilitate an increased hydraulic radius and to help reduce the confinement in the pillar to facilitate caving when resuming mining from level 1079.

Based on the progress in development, drilling and associated production activities, production is planned to be resumed on level 1079 by Q3 2022. The production is planned to start in the damaged Y17–Y25 area in mid-Q3 and depending on the production rate, the undercut is expected to be finished by the end of Q2, 2023 (4 kt/day) or the end of Q4, 2023 (2 kt/day). The production rate vary depending upon the frequency of operational and production issues during mining. Hence, draw control and cave management is essential to maintain an optimal cave front through regular mine plan compliance checks and necessary actions to mine as close as possible to the analysed mine plans.

Acknowledgement

The authors greatly acknowledge LKAB for permission to publish the result of this project.

References

Dahnér, C, Malmgren, L & Boskovic, M 2008, 'Possible causes of course of events at February 2, 2008', LKAB Internal report, 08–769.

Ghazvinian, E, Garza-Cruz, T, Bouzeran, L, Fuenzalida, M, Cheng, Z, Cancino, C & Pierce, M 2020, 'Theory and Implementation of the Itasca Constitutive Model for Advanced Strain Softening (IMASS)', in R Castro, F Báez & K Suzuki (eds), *Proceedings of the Eighth International Conference & Exhibition on Mass Mining (MASSMIN 2020),* University of Chile, Santiago, pp. 451–461.

Hebert, Y & Sharrock, G 2018, 'Three-dimensional simulation of cave initiation, propagation and surface subsidence using a coupled finite difference–cellular automata solution', in Y Potvin & J Jakubec (eds), *Proceedings of the Fourth International Symposium on Block and Sublevel Caving,* Australian Centre for Geomechanics, Perth, pp. 151–166, https://doi.org/10.36487/ACG_ rep /1815_09_Hebert

Itasca 2021, *FLAC3D (Fast Lagrangian Analysis of Continua 3D)*, Version 7.0, computer software, Minneapolis: Itasca Consulting Group, Inc., http://www.itascacg.com/software/FLAC3D

Malovichko, D 2021. 'Kiruna Mine: Analysis of Seismic Data Related to the Large Event on 18 May 2020 Task 1A: Finite Source Inversion of the Mainshock', 2021/04/12 – Report KIRUNA-REP-LRGEVENT-202005-DM. Report by Institute of Mine Seismology.

Sandström, D 2003. *Analysis of the Virgin State of Stress at the Kiirunavaara Mine*, Licentiate Thesis 2003:02, Luleå Tekniska Universitet, Sweden. ISSN:1402–1757.

Sharrock, G 2021, *CAVESIM Users manual,* Version 6.5. Itasca Australia Pty Ltd, Australia.